Anal. Chem. **2010,** *82,* 3343–3351

Ultrashort Separation Length Homogeneous Electrophoretic Immunoassays Using On-Chip Discontinuous Polyacrylamide Gels

Chenlu Hou[†] and Amy E. Herr*[,‡]

Department of Electrical Engineering and Computer Science and Department of Bioengineering, University of California, Berkeley 94720

To realize efficient homogeneous electrophoretic immunoassays, we introduce discontinuous polyacrylamide gels that enable quantitative assay completion in separation lengths as short as 350 μm in <10 s. The discontinuous cross-linked gels reduce the required electrophoretic separation lengths and thereby significantly reduce the required applied electrical potentials needed to achieve 100's V/cm electric field strengths for rapid electrophoresis. To optimize the discontinuous polyacrylamide gel assay format, we demonstrate development of a two-color homogeneous electrophoretic immunoassay for concurrent quantitation of C reactive protein (CRP) and tumor necrosis factor-α (TNF-α) for monitoring inflammatory response. To achieve necessary pore-size control at the gel discontinuity, an optimized mask-based fabrication protocol is introduced. The fabrication approach improves electrophoretic separations using the discontinuous separation gels by eliminating two confounding phenomena: (1) smaller than desired pores at the discontinuity which result in undesired physical exclusion of large-species and (2) an associated transition from small to large pores aft of the interface which acts to "destack" analyte bands during the separation. With the use of the optimized discontinuous separation gels, both assays were linear and quantitative over a two-log detection range, with a lower limit of detection of 11 ng/mL for CRP and 40 ng/mL for TNF-α. An optimal single-point detector location was identified by balancing the separation resolution and assay duration constraints. The ultrashort separation distance electrophoretic assays developed here provide flexibility in chip and instrument design by relaxing electrical potential requirements and expanding the possibilities for assay multiplexing, therefore addressing important design considerations when developing field-portable diagnostic assays for near-patient environments.

Homogeneous electrophoretic immunoassays are well-suited for and often employed as clinical diagnostics. While heterogeneous immunoassays require surface immobilization of a capture probe or multiple washing steps for high specificity,[1−3] the homogeneous format utilizes electrophoresis to separate immune complexes and unbound affinity probes. Elimination of surface immobilization and washing steps simplifies assay implementation and reduces reagent consumption. When implemented with technologies including microfluidics, the assays become amenable for use in point-of-care settings.[4−6] In conjunction with a lab-on-a-chip format, automated operation of the immunoassays is conducive to single device integration of upstream sample preparation (i.e., mixing, incubation of probe with sample matrix, analyte enrichment).[7,8] Further, microfluidic homogeneous electrophoretic immunoassays support concurrent multianalyte and/or multisample analysis.[9−12] Nevertheless, while microfluidic technology affords sophisticated, multistage analyses with quick reporting of results, the portability and field adaptability of electrophoretic immunoassays are limited in part by the need for high-voltage power supplies. Thus, a reduction in the required separation length would, in turn, reduce applied electrical potential (voltage) constraints, while allowing high electric field strength operation.

Both direct and competitive homogeneous immunoassays use the formation of immune complexes to indicate the concentration of target protein in a sample.[13] Native conditions facilitate formation of immune complexes but present a challenge to electrophoresis as the resulting immune complexes and unbound

* To whom correspondence should be addressed. Phone: (510) 666-3396. Fax: (510) 642-5835. E-mail: aeh@berkeley.edu.
† Department of Electrical Engineering and Computer Science.
‡ Department of Bioengineering.

(1) Hosokawa, K.; Omata, M.; Sato, K.; Maeda, M. *Lab Chip* **2006**, *6*, 236–241.
(2) Gervais, L.; Delamarche, E. *Lab Chip* **2009**, *9*, 3330–3337.
(3) Fan, R.; Vermesh, O.; Srivastava, A.; Yen, B. K. H.; Qin, L. D.; Ahmad, H.; Kwong, G. A.; Liu, C. C.; Gould, J.; Hood, L.; Heath, J. R. *Nat. Biotechnol.* **2008**, *26*, 1373–1378.
(4) Verpoorte, E. *Electrophoresis* **2002**, *23*, 677–712.
(5) Amundsen, L. K.; Siren, H. *Electrophoresis* **2007**, *28*, 99–113.
(6) Hou, C.; Herr, A. E. *Electrophoresis* **2008**, *29*, 3306–3319.
(7) Kawabata, T.; Wada, H. G.; Watanabe, M.; Satomura, S. *Electrophoresis* **2008**, *29*, 1399–1406.
(8) Herr, A. E.; Hatch, A. V.; Throckmorton, D. J.; Tran, H. M.; Brennan, J. S.; Giannobile, W. V.; Singh, A. K. *Proc. Natl. Acad. Sci. U.S.A.* **2007**, *104*, 5268–5273.
(9) Cheng, S. B.; Skinner, C. D.; Taylor, J.; Attiya, S.; Lee, W. E.; Picelli, G.; Harrison, D. J. *Anal. Chem.* **2001**, *73*, 1472–1479.
(10) Dishinger, J. F.; Reid, K. R.; Kennedy, R. T. *Anal. Chem.* **2009**, *81*, 3119–3127.
(11) Bromberg, A.; Mathies, R. A. *Electrophoresis* **2004**, *25*, 1895–1900.
(12) Kawabata, T.; Watanabe, M.; Nakamura, K.; Satomura, S. *Anal. Chem.* **2005**, *77*, 5579–5582.
(13) Yeung, W. S. B.; Luo, G. A.; Wang, Q. G.; Ou, J. P. *J. Chromatogr., B* **2003**, *797*, 217–228.

10.1021/ac100182j
Published on Web 03/24/2010

antibodies possess similar charge-to-mass ratios.[14] As a result, on-chip competitive immunoassays relying on separation of labeled antigen (instead of antibodies) from the immune complex are applied toward detecting small hormones,[15−17] drug molecules,[18] and proteins.[10,19,20] Despite the challenge presented by separation, direct immunoassays are desirable due to straightforward implementation and often superior sensitivity.[21] While a recent review by the authors of this study summarizes on-chip electrophoretic immunoassay developments,[6] highlighted here are the state-of-the-art approaches to shorten direct immunoassay separation lengths. To sharpen peaks and enhance mobility differences between resolving species, a recent approach uses the high charge-to-mass ratio of DNA to mask antibody Fab fragment charge heterogeneity by conjugating DNA to Fab fragments.[7,12,22] With the use of the approach, antiprostate specific antigen (PSA) Fab coupled with 245-bp DNA was resolved from the PSA-Fab-DNA complex in ~1 cm using the Agilent 2100 Bioanalyzer.[12] In comparison, coupling 626-bp DNA to anti-α-fetoprotein (AFP) Fab was less successful and required formation of a sandwich immune complex with an additional antibody to fully resolve the immune complex. Electrophoretic immunoassays completed in millimeters-long separation lengths have also been reported using bulk flow, including electroosmosis and pressure driven flow, to counteract electrophoresis.[23,24] A gradient elution moving boundary electrophoresis (GEMBE) assay enabled electrophoretic immunoassays for protein kinase A in 3 mm separation lengths.[23] During separation, a pressure and electroosmotic-driven buffer counter flow was gradually decreased, thus allowing elution of target analytes one-by-one into a capillary in order of decreasing electrophoretic mobility. Detection was accomplished by monitoring either a step increase in fluorescence passing by a single-point detector[25] or a change in channel current[23] (which indicated entry of new target analyte into the channel). The detection approach obviates the need to spatially resolve analytes into individual bands, as is required in conventional electrophoresis. Lastly, techniques such as spectral multiplexing and concurrent two-color detection[26] as well as affinity reagent mobility adjustment[12,27] enabled development of simultaneous immunoassays in a single separation channel without increasing separation length or chip footprint.

Microfluidic formats incorporating in situ sieving matrices have also improved electrophoretic immunoassay performance and have been implemented in a wide range of formats (i.e., cross-linked gels,[8,28,29] noncross-linked gels,[7,22,30] nanofabricated structures[24]). Sieving matrices enhance mobility differences among analytes and can be optimized by tuning the pore-size while eliminating bulk flow and minimizing nonspecific adsorption. With the use of 1% methylcellulose as a sieving matrix, a competitive immunoassay toward human serum albumin resolved species in a separation length of 1 cm at 300 V/cm.[30] In a different approach to sieving matrices, two-dimensional nanosieving arrays with anisotropically etched trenches resolved large immune complexes from smaller antibodies in a 400 μm × 1 mm subregion of a 5 mm × 5 mm chamber.[24] In yet a different approach, photopatterned cross-linked gels yield nanoporous sieving structures without dedicated nanofabrication facilities. Photopolymerization enables spatial control of characteristics such as gel pore-size and pore-size gradients, thus allowing optimization of separation performance and integration of preparatory functionality.

Use of uniform pore-size polyacrylamide (PA) gels was demonstrated by our group and others for protein sizing and homogeneous immunoassays.[28,29,31] Direct assays for tetanus antibody and competitive assays for tetanus toxin were completed in an effective separation length of 6 mm at 300 V/cm.[28] Also, with the use of uniform pore-size PA gels, ricin toxin was quantified with an effective separation length of 5 mm;[29] however, an overlap of toxin−antibody complex peak and antibody peak at the detection point suggests separation performance for ricin detection could be further improved through, for example, spatially tuning the pore-size of the sieving matrix. While homogeneous electrophoretic immunoassays in gradient gels have not been reported, protein sizing using gradient pore-size gels and pore limit gel electrophoresis have shown promise.[32,33] A microscale gradient gel with a large-to-small pore-size distribution in the separation channel resolved SDS-treated proteins with molecular weights ranging from 20 to 205 kDa in a separation length of 4 mm at 298 V/cm.[32] Just as in the slab-gel macroscale counterpart, decreasing pore-size gradients impart additional resolution and sensitivity as species migrating along the separation axis continuously sharpen. While microchip discontinuous (stacking) gels have been previously described for microfluidic DNA[34] and protein sizing,[35,36] no known efforts exist to harness the format for ultrashort separation length electrophoretic immunoassays.

We present development, optimization, and demonstration of electrophoretic immunoassays conducted on discontinuous PA sieving gels. Optimization of discontinuous gels enables baseline resolution of antibody and immune complex in <450 μm, an order

(14) Ou, J. P.; Wang, Q. G.; Cheung, T. M.; Chan, S. T. H.; Yeung, W. S. B. *J. Chromatogr., B* **1999**, *727*, 63–71.
(15) Koutny, L. B.; Schmalzing, D.; Taylor, T. A.; Fuchs, M. *Anal. Chem.* **1996**, *68*, 18–22.
(16) Schmalzing, D.; Koutny, L. B.; Taylor, T. A.; Nashabeh, W.; Fuchs, M. *J. Chromatogr., B* **1997**, *697*, 175–180.
(17) Taylor, J.; Picelli, G.; Harrison, D. J. *Electrophoresis* **2001**, *22*, 3699–3708.
(18) Chiem, N.; Harrison, D. J. *Anal. Chem.* **1997**, *69*, 373–378.
(19) Roper, M. G.; Shackman, J. G.; Dahlgren, G. M.; Kennedy, R. T. *Anal. Chem.* **2003**, *75*, 4711–4717.
(20) Dishinger, J. F.; Kennedy, R. T. *Anal. Chem.* **2007**, *79*, 947–954.
(21) Heegaard, N. H. H.; Kennedy, R. T. *J. Chromatogr., B: Anal. Technol. Biomed. Life Sci.* **2002**, *768*, 93–103.
(22) Park, C. C.; Kazakova, I.; Kawabata, T.; Spaid, M.; Chien, R. L.; Wada, H. G.; Satomura, S. *Anal. Chem.* **2008**, *80*, 808–814.
(23) Ross, D.; Kralj, J. G. *Anal. Chem.* **2008**, *80*, 9467–9474.
(24) Yamada, M.; Mao, P.; Fu, J. P.; Han, J. Y. *Anal. Chem.* **2009**, *81*, 7067–7074.
(25) Shackman, J. G.; Munson, M. S.; Ross, D. *Anal. Chem.* **2007**, *79*, 565–571.
(26) Guillo, C.; Roper, M. G. *Electrophoresis* **2008**, *29*, 410–416.
(27) Yang, P. L.; Whelan, R. J.; Mao, Y. W.; Lee, A. W. M.; Carter-Su, C.; Kennedy, R. T. *Anal. Chem.* **2007**, *79*, 1690–1695.
(28) Herr, A. E.; Throckmorton, D. J.; Davenport, A. A.; Singh, A. K. *Anal. Chem.* **2005**, *77*, 585–590.
(29) Meagher, R. J.; Hatch, A. V.; Renzi, R. F.; Singh, A. K. *Lab Chip* **2008**, *8*, 2046–2053.
(30) Mohamadi, M. R.; Kaji, N.; Tokeshi, M.; Baba, Y. *Anal. Chem.* **2007**, *79*, 3667–3672.
(31) Herr, A. E.; Singh, A. K. *Anal. Chem.* **2004**, *76*, 4727–4733.
(32) Lo, C. T.; Throckmorton, D. J.; Singh, A. K.; Herr, A. E. *Lab Chip* **2008**, *8*, 1273–1279.
(33) Sommer, G. J.; Singh, A. K.; Hatch, A. V. *Lab Chip* **2009**, *9*, 2729–2737.
(34) Brahmasandra, S. N.; Ugaz, V. M.; Burke, D. T.; Mastrangelo, C. H.; Burns, M. A. *Electrophoresis* **2001**, *22*, 300–311.
(35) Das, C.; Zhang, J.; Denslow, N. D.; Fan, Z. H. *Lab Chip* **2007**, *7*, 1806–1812.
(36) Yang, S.; Liu, J. K.; Lee, C. S.; Devoe, D. L. *Lab Chip* **2009**, *9*, 592–599.

of magnitude shorter than previous work. Additionally, simultaneous assays for quantitation of the proteins C reactive protein (CRP) and tumor necrosis factor-α (TNF-α) are developed using the discontinuous PA gels and two-color detection. Both proteins are important components of inflammation and host response.[37−39] Characterization of the immunoassays in uniform pore-size gels, gradient pore-size gels, and discontinuous pore-size PA gels is performed. During optimization, we introduce a new fabrication technique to eliminate protein exclusion and "destacking" dispersion associated with previously reported on-chip discontinuous gels.[28,36] These results form the basis for our ongoing work to develop field-portable diagnostic instruments for use in near-patient environments without the need for specialized, expensive high-voltage power supplies. Further, the efficient homogeneous electrophoretic immunoassays detailed here are multiplexed and conducted in a compact microfluidic format, as is relevant to near-patient monitoring of protein biomarker panels including markers of infection and inflammation.

MATERIALS AND METHODS

Reagents. Solutions of 30% (29:1) acrylamide/bis-acrylamide, 3-(trimethoxysilyl)-propyl methacrylate (98%), glacial acetic acid, 2-hydroxyethyl cellulose, and methanol were purchased from Sigma Aldrich (St. Louis, MO). Photoinitiator 2,2-azobis[2-methyl-*N*-(2-hydroxyethyl) propionamide] (VA-086) was purchased from Wako Chemical (Richmond, VA). Monoclonal CRP antibody was purchased from Abcam (Cambridge, MA). Monoclonal TNF-α antibody was purchased from Meridian Life Science (Saco, ME). Purified human serum CRP was purchased from Calbiochem (San Diego, CA), and recombinant TNF-α protein was purchased from R&D Systems (Minneapolis, MN). Alexa Fluor 488 conjugated trypsin inhibitor (TI) was purchased from Invitrogen (Carlsbad, CA) and used as an assay internal standard for peak height and mobility. Bovine serum albumin (BSA) was purchased from Sigma. TNF-α antibody (anti-TNF-α Ab) and CRP antibody (anti-CRP Ab) were fluorescently labeled in-house using Alexa Fluor 488 and 568 antibody labeling kits (Invitrogen, Carlsbad, CA), respectively. Fluorescently labeled species are noted with an asterisk (*) in this study. Tris-glycine (10×) native electrophoresis buffer (pH 8.3, 0.25 M Tris, 1.92 M glycine) was purchased from Bio-Rad Laboratories (Hercules, CA).

Protein Samples. TI*, anti-TNF-α Ab*, anti-CRP Ab*, CRP, and TNF-α were prepared in 1× native Tris-glycine buffer. For two-color immunoassays, the TI*, anti-TNF-α Ab*, and anti-CRP Ab* concentrations were held constant ([TI*] = 50 nM, [Ab_{TNF}*] = 68 nM, [Ab_{CRP}*] = 66 nM) while the CRP and TNF-α concentrations were varied among the different samples. All samples were adjusted to a final volume of 20 μL with 1× native Tris-glycine buffer. Samples were mixed in plastic tubes by gentle vortexing for 10 s and incubated at 4 °C for at least 1 h. To minimize protein loss due to nonspecific binding, all tube surfaces were blocked by preincubation of tubes with a 5% (w/v) BSA solution, which was removed prior to sample introduction.

Glass Chip Fabrication and Surface Preparation. Glass microfluidic chips with simple t-channel networks were fabricated using standard wet etch processes by Caliper Life Sciences (Hopkinton, MA). Channels were ∼20 μm deep and ∼90 μm wide. To enable covalent attachment of the PA gel to channel walls, microchannels were coated with a self-assembled silane monolayer.[31] Bare channels were first incubated with 1 M NaOH for 10 min, flushed with house DI water, and then purged by vacuum. A degassed 2:3:5 (v/v/v) mixture of 3-(trimethoxysilyl)-propyl methacrylate, glacial acetic acid, and DI water was then introduced into the channels via capillary flow for silane monolayer formation. Following a 30 min incubation, the channels were rinsed for 10 min with methanol and DI water and purged with vacuum.

Loading and Separation Gels. Three separation gel formats were used to optimize electrophoretic immunoassay performance: (1) uniform pore-size gels, (2) pore-size gradient gels (large-to-small pores), and (3) discontinuous pore-size gels. The first two formats are used to benchmark and optimize the new discontinuous PA gel format. PA gel precursor solutions of the appropriate acrylamide concentration (*T*) were prepared by diluting 30% (w/v) acrylamide/bis-acrylamide solution with Tris-glycine native electrophoresis buffer to a total volume containing 0.2% (w/v) VA-086 photoinitiator. Precursor solutions were vigorously sonicated and degassed prior to use, as is critical to ensure a void-free PA gel. For all formats, a large pore-size gel (2.5%T) in the loading channel was used to allow rapid, nonbiased loading of all species to the injection junction, while suppressing bulk fluid flow. A 2.5%T large pore-size loading gel was chosen, as PA has been observed to fail to cross-link at ≤2%T.[40] An 8%T minimum pore-size gel was chosen as immune complexes studied here exhibit size exclusion from smaller pore-size PA gels.

Gel Fabrication: Uniform and Decreasing Pore-Size Gradient Gels. Uniform and decreasing pore-size gradient gels have been reported previously for protein sizing[31,32] and electrophoretic immunoassays[8,28,29] and are used here to benchmark performance for the discontinuous gel format. Briefly, the following protocol was used to fabricate uniform separation gels: gel precursor solution was wicked into all channels, the chip was aligned to a UV light source 18 cm away (10 mW/cm^2 at the plane of the chip), and finally the chip was exposed for 8 min via flood exposure to a fan-cooled, spectrally filtered mercury lamp (300−380 nm, 100 W, UVP, B100-AP, Upland, CA). To fabricate 2.5%T-to-8%T gradient pore-size gels, the following protocol was used: high percentage acrylamide gel precursor solution (8%T) was introduced into all channels, a 6 min exposure to UV (fan-cooled 100 W mercury lamp 16 cm away, 12 mW/cm^2 at chip plane) with photomasking yielded a gel plug at the end of the separation channel, unpolymerized high-percentage acrylamide gel precursor solution in the loading channel was flushed out and replaced with low-percentage gel acrylamide precursor solution (2.5%T), a gradient-generating diffusion period of 5 min ensued, and last an 8 min flood UV exposure of the entire chip at 10 mW/cm^2 was completed. Consequently, the loading channel housed a large pore-size (2.5%T) PA gel and the separation channel housed a large-to-small pore-size PA gel gradient (i.e., 2.5%T-to-8%T).

(37) Ridker, P. M.; Hennekens, C. H.; Buring, J. E.; Rifai, N. *N. Engl. J. Med.* **2000**, *342*, 836–843.
(38) Ulloa, L.; Tracey, K. J. *Trends Mol. Med.* **2005**, *11*, 56–63.
(39) Kishore, U.; Gaboriaud, C.; Waters, P.; Shrive, A. K.; Greenhough, T. J.; Reid, K. B. M.; Sim, R. B.; Arlaud, G. J. *Trends Immunol.* **2004**, *25*, 551–561.
(40) Hedrick, J. L.; Smith, A. J. *Arch. Biochem. Biophys.* **1968**, *126*, 155–164.

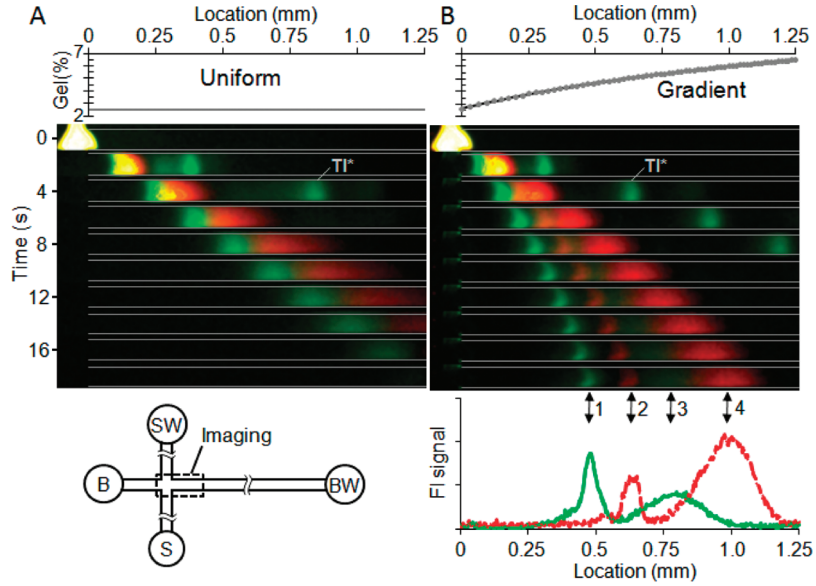

Figure 1. Implementation of a pore-size gradient in the separation gel allows two-color assay completion in 1 mm. CRP (red channel) and TNF-α (green channel) assay on a double-T chip with 2.5%T uniform gel (A) and 2.5%T−8%T gradient gel (fabricated in situ) (B). $E = 102$ V/cm. Labels indicate (1) TNF complex; (2) CRP complex; (3) anti-TNF Ab*; (4) anti-CRP Ab*. The spatially varying effective PA pore-size is shown on the top panel, as determined by mobility calibration for anti-CRP Ab* (see Materials and Methods). Fluorescence intensity profiles are shown at 18 s for the immunoassay implemented in gradient gel (B, bottom panel). [TI*] = 50 nM, [anti-CRP Ab*] = 66 nM, [CRP] = 16 nM, [anti-TNF-α Ab*] = 68 nM, and [TNF-α] = 22 nM.

Gel Fabrication: Discontinuous Pore-Size Gels. The third format consisted of a large-to-small pore-size gel discontinuity located at the start of the separation channel. The format is similar in concept to stacking gels used in slab-gel formats, with the caveat that here the discontinuity was included so as to differentially retard the migration of large immune complexes relative to the smaller free antibody, with a secondary performance benefit stemming from the "stacking" effect of the slowed migration of both species. Further, the buffer system used for the homogeneous immunoassays was a uniform buffer system. To fabricate discontinuous pore-size gels, the following protocol was used: the chip was aligned to a transparency mask (designed in house and fabricated by Fineline Imaging, Colorado Springs, CO) exposing the separation channel to UV illumination from an Olympus IX-50 microscope equipped with a 100 W mercury arc lamp and a 4× UV objective (UPLANS-APO, NA = 0.16); after alignment, the separation gel precursor solution ($T = 2.5$, 3.5, 4, 5, 6 or 8%) was wicked into all channels and excess precursor solution was removed from channel reservoirs; drops of high viscosity 5% (w/v) 2-hydroxyethyl cellulose (HEC) were applied to each reservoir and equilibrated for 10 min to yield quiescent flow conditions; the precursor filled microchannels were then exposed to UV excitation for a set duration (see Results and Discussion for details on fabrication optimization); unpolymerized separation gel precursor solution in the loading channel was then flushed out and replaced with loading gel precursor solution (2.5%T) via pressure driven flow; and finally the unmasked chip was flood exposed for 8 min on a 100 W UV lamp (10 mW/cm^2).

APPARATUS AND IMAGING

Chip Hardware. The sample (S), sample waste (SW), buffer (B), and buffer waste (BW) reservoirs are indicated in Figure 1A. The distances from chip intersection to S, SW, B, and BW reservoirs are 0.39, 1.51, 0.74, and 4.56 cm, respectively. An in-house machined manifold clamped the chip between a Delrin top housing and an aluminum frame; O-rings in the top housing sealed around the chip reservoirs. The SW, B, and BW reservoirs were filled with 50 μL of 1× native Tris-glycine buffer and 5 μL of protein sample filled the S reservoir. Voltage was applied using a programmable high-voltage power supply (LabSmith, Livermore, CA) and platinum electrodes were inserted into the top manifold reservoirs. Samples were electrophoretically loaded for 2 min by applying 450 V to SW while grounding the S, B, and BW reservoirs ($E = 160$ V/cm in the loading channel).

Full-Field Imaging. Images were collected using an inverted epi-fluorescence microscope (Olympus IX-70) equipped with a 100 W mercury arc lamp, a 10× objective, and a Peltier-cooled charge-coupled device (CCD) camera (CoolSNAP HQ2, Roper Scientific, Trenton, NJ). Dual color CCD imaging relied on the use of two filter cubes and independent realizations of separations in each color signal. To produce two-color CCD images, image sequences collected on one spectral channel (AF 488 with Omega Optical GFP filter cube) were summed with image sequences taken on the second spectral channel (AF 568 with Omega Optical dsRed2 filter cube) from back-to-back injections of the same multicomponent samples. A 0.63× demagnifier (Diagnostic Instruments Inc., Sterling Heights, MI) was used to increase the field of view projected onto the CCD. Unless otherwise stated, the CCD exposure time was 150 ms. Prior to separation, the voltage program used −100 V applied to the BW reservoir for 10 s to form a symmetrical pinched injection plug. Separation was initiated by applying 800 V to BW, grounding B, 400 V to S, and 600 V to SW to inject a well-defined "pinched" sample plug. The resulting electric field strength in the separation channel was $E = 102$ V/cm. With the use of ImageJ (NIH) for postprocessing, CCD images collected allowed calculation of analyte migration distance

and peak width from which protein mobility and separation resolution were derived.

Single-Point, Two-Color Concurrent Detection. Simultaneous immunoassays were completed in a single separation channel using single-point two-color detection. Quantitation of TNF-α and CRP utilized a custom filter cube on an IX-70 microscope and a two-channel photomultiplier tube (PMT) detection system (Photon Technology International) mounted to the IX-70. Mercury arc lamp excitation was spectrally filtered with a 490 and 577 nm dual band excitation filter (XF1051, Omega Optical) and reflected off a dichroic mirror (490 and 575 nm notch filter, XF2044 by Omega Optical). A 40× objective (NA = 0.60) focused on the separation channel defined the detection point. Fluorescence was spatially filtered (iris) prior to PMT detection. A dichroic mirror (560 nm long pass, XF2017 by Omega Optical) split the fluorophore emissions into red and green channels. Each channel was further filtered by individual emission filters (XF3081 and XF3301, Omega Optical) to minimize crosstalk. Fluorescence intensity at the detector was normalized by the fluorescence intensity of the two-color sample in the loading channel prior to the separation. Signals from the PMTs were collected via a data acquisition board, and electropherograms were generated using an in-house LabView program.

To increase the separation electric field for the single-point detection assays, a modified voltage program was used. An upper limit on the electric field was set by gel breakdown observed when $E > 500$ V/cm for an extended duration. The maximum field constraint most directly impacted the short channel segment connecting the injection junction to B during the separation phase, thus a two-step pull-back voltage scheme was utilized. To inject a tight plug into the separation channel and limit injection leakage, for the first 5.5 s of the separation 800 V was applied to BW, B was grounded, S was set to 400 V, and SW was set to 600 V. Thereafter, 1100 V was applied to BW while the S and SW voltages were set to 195 and 220 V, respectively. The resulting separation electric field was 200 V/cm with the channel segment B to the injection junction set at 250 V/cm, well under the gel breakdown limit.

Uniform Gels for Electrophoretic Mobility Calibration. Characterization of gel pore-size along the separation axis followed previously described approaches.[32] Briefly, electrophoretic mobility (μ) as a function of migration distance (L) was extracted from CCD separation image time sequences. The time-derivative of the migration distance divided by the applied electric field yielded mobility ($\mu = (1/E)(\partial L/\partial t)$). To calibrate the relationship between unknown gel pore-size and measured protein mobility, anti-CRP Ab* mobility was measured in five uniform pore-size PA gels (2.5%T, 3.5%T, 4%T, 5%T, 6%T). Calibration yielded a log-linear relationship between gel pore-size and apparent electrophoretic mobility: $\log(\text{mobility, cm}^2/(\text{V s})) = -(0.111T) - 3.71$ ($R^2 = 0.974$).

Calculation of Separation Resolution. The ability to distinguish two peaks is quantified by the separation resolution (SR), which is defined as the ratio of peak-to-peak separation distance (ΔL) to peak width (4σ).[41] While SR ≥ 1.5 indicates two completely resolved peaks (baseline resolution), SR = 1 is more than adequate to indicate separation completion and here employed as a performance metric. To obtain SR during each electrophoretic immunoassay, a built-in least-squares fitting algorithm in MATLAB (MathWorks, Natick, MA) and an in-house multipeak Gaussian fitting script were used to identify peak location and peak variance at each time point.

RESULTS AND DISCUSSION

Homogeneous Electrophoretic Immunoassays in PA Sieving Gels. To benchmark performance among various separation gel formats, the minimum separation length required for homogeneous electrophoretic immunoassays under full-field imaging is defined by the peak front of the antibody (probe) when SR between the probe and the immune complex exceeds unity. Assuming a Gaussian concentration profile ($C(x) = C_m e^{-\{(x-L)^2/(2\sigma^2)\}}$), the antibody peak front is the sum of antibody migration distance and peak half-width ($L_{Ab} + 2\sigma_{Ab}$). To provide context for how the sieving matrix composition affects separation length, SR is here derived as a function of antibody migration distance (L_{Ab}) assuming uniform electric field and electrophoretic mobility. First, peak-to-peak distance between the immune complex and free antibody (ΔL) is directly proportional to the mobility difference between the two species: $\Delta L = (\Delta\mu/\mu_{Ab})L_{Ab}$. Mobility ($\mu$) and differential mobility ($\Delta\mu/\mu$) are a function of PA gel composition according to the Ferguson relationship:[42] $\mu_{Ab} = \mu_0 10^{-K_{Ab}T}$ and $\mu_{complex} = \mu_0 10^{-K_{complex}T}$. Here K_{Ab} and $K_{complex}$ are the antibody and complex retardation coefficients, respectively, and T is the total acrylamide concentration in the PA gel precursor solution. The differential mobility ($\Delta\mu/\mu$), expressed as $(\Delta\mu/\mu_{Ab}) = 1 - 10^{-(K_{complex} - K_{Ab})T}$, increases with T as the complex has a greater retardation coefficient than the smaller antibody. Another factor determining SR is the analyte peak width, which increases due to diffusion: $\sigma = (\sigma_0^2 + 2Dt)^{1/2}$, where σ_0 is the injected peak width, D is the diffusion coefficient, and t is the elapsed separation time. Substituting $t = L_{Ab}/(\mu_{ab}E)$ relates the peak width to separation length: $\sigma = [\sigma_0^2 + 2(D/\mu_{Ab})(L_{Ab}/E)]^{1/2}$. When altering gel pore-size, D changes with μ since migration by electrophoresis and diffusion encounter the same drag force.[43] Therefore, increasing T or decreasing the PA gel pore-size yields an increased SR at a given migration distance (L_{Ab}). A trade-off exists, however, as decreasing the PA gel pore-size results in slower migration velocities and thus longer assay duration when using single-point detection. Tuning of the gel pore-size allows assay developers to maximize the SR while minimizing the separation length ($L_{Ab} + 2\sigma_{Ab}$) and assay duration. Practical considerations require large pore-size gels in the loading channel to allow unbiased introduction of even large species (i.e., CRP complex ~175 kDa, TNF-α complex ~200 kDa).

Uniform and Gradient Gels. Comparison of separation performance between uniform 2.5%T separation gels and 2.5%T-to-8%T decreasing pore-size gradient gels is detailed in Table 1. The uniform large pore-size gel did not resolve the immune complex from the antibody probe within the first millimeter of

(41) Giddings, J. C. *Unified Separation Science*; John Wiley & Sons, Inc.: New York, 1991.

(42) Ferguson, K. A. *Metab., Clin. Exp.* **1964**, *13*, 985–1002.

(43) Ornstein, L. *Ann. N.Y. Acad. Sci.* **1964**, *121*, 321–349.

Table 1. Optimization of Polyacrylamide Gel Format for CRP Immunoassay

	uniform	gradient	discontinuous				
gel architecture	2.5%T	2.5%T-to-8%T	2.5/2.5	2.5/3.5	2.5/4.0	2.5/5.0	2.5/6.0
$\Delta\mu/\mu_{Ab^*}$ in separation gel	<5%	varies	7.3%	52%	68%	79%	85%
Ab* migration distance ($L_{\text{anti-CRP Ab}^*}$) for SR ≥ 1 [μm]	>4000	750	>3000	850	515	320	285
separation length ($L_{\text{anti-CRP Ab}^*} + 2\sigma_{\text{anti-CRP Ab}^*}$) for SR ≥ 1 [$\mu$m]	>4000	925	>3000	1080	650	390	335
elapsed separation time for SR > 1 [s]		12.2		10.9	6.3	5.6	5.2

separation length (Figure 1A) and ultimately required >4 mm of separation length, as was expected. Use of the gradient gel (Figure 1B) yielded SR > 1 for the CRP assay in a separation length of 925 μm. To achieve SR > 1, the assay duration was 12.2 s (E = 102 V/cm). The gradient gel yielded separation of anti-TNF-α from the immune complex in 850 μm ($L_{\text{anti-TNF Ab}^*} + 2\sigma_{\text{anti-TNF Ab}^*}$) with assay completion in 14.5 s (E = 102 V/cm). On the basis of these rapid separation times, serial analysis of two or more analyte targets in a single sample, in a single channel is possible in less than 1 min. Further, the short separation distances required in the gradient gel indicate that a 1 mm separation channel would likely be sufficient for both of the homogeneous electrophoretic assays conducted.

As is evident in Figure 1, the mobility difference between the free antibody and the larger immune complex is notably enhanced on the gradient gel, as compared to the uniform large pore-size gel. Nevertheless, electrophoretic immunoassays for CRP using the gradient gel reveal that effective immunoassay separations were not achieved until species migrated into a pore-size region with T > 4%. Thus, the first 500 μm of the 2.5%T-to-8%T decreasing pore-size gradient gel was ineffective at resolving the immune complexes from free antibody. While the gradient format can effectively resolve a wide molecular weight range of proteins, the gradient gel is not optimized for homogeneous immunoassays that require resolution of just a handful of species within a well-defined molecular weight range. These results suggest that increasing the slope of the pore-size gradient or, equivalently, locating a small pore-size (>4%T) region proximal to the injection junction would reduce the required separation length and allow design of a more compact device.

Development of a Discontinuous Gel Format. The following sections detail development, fabrication, and optimization of discontinuous PA gels for homogeneous electrophoretic immunoassays.

Spatial Control of Gel Pore-Size at the Discontinuity. Fabrication of an abrupt large-to-small pore-size transition in the separation channel (noted as 2.5/5%T) required adjustment and optimization of a mask-based partial illumination photolithography technique.[31] The nominal location of the gel pore-size discontinuity was controlled by mask alignment to the separation channel. Initial fabrication using the partial illumination technique with the IX-50 mercury lamp and UV objective as the illumination source yielded a nonideal pore-size distribution at the discontinuity (Figure 2A), as has been observed by our group and collaborators previously.[28] Assessment of anti-CRP Ab* migration velocity along the separation axis revealed a smaller than expected pore-size at the PA 2.5/5%T gel interface. On the basis of mobility calibration data, an apparent pore-size of 9%T was observed instead of the desired 5%T PA gel. The 2.5%/5%T gel discontinuity acted to exclude CRP immune complex despite observations that uniform 5%T PA gels

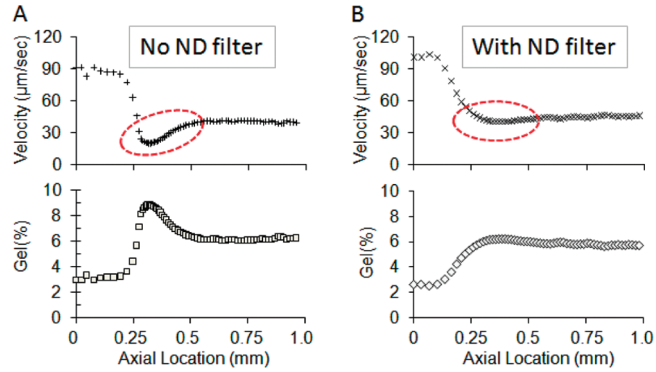

Figure 2. Fabrication of PA gel pore-size discontinuity is strongly dependent on exposure intensity using partial illumination (mask-based) patterning. (A) No neutral density filter used for fabrication of discontinuous gel interface results in poorly controlled pore-size distribution. Exposure time: 3 min, power = ~600 mW/cm^2. (B) Neutral density filter used to decrease illumination power results in more well-controlled pore-size distribution at discontinuity. Exposure time, 3.3 min; power = 7.5 mW/cm^2. Both gels are 2.5/5% discontinuous gels; loading gel (2.5%) fabrication exposure was the same in both cases. Pore-size determined via anti-CRP Ab* mobility tracking.

fabricated with flood illumination (no mask-based photopatterning) allowed free migration of immune complex (data not shown). Additionally, significant dispersion ("destacking") of the Ab* peak was observed during the first 300 μm aft of the gel discontinuity. In this region, mobility calibration revealed that the apparent pore-size increased from that of a 9%T gel to that of a 6%T PA gel thus resulting in band "destacking". Similar destacking effects were observed in microfluidic proteomic assays using discontinuous gels[36] and were addressed with usage of a discontinuous buffer system for band sharpening.

Theoretical modeling suggests that UV photopolymerization under partial illumination can result in nonideal pore-size variation near the polymer/precursor interface.[44] The mechanism stems from a monomer concentration gradient established across the masked region to the exposed region during the photopolymerization process. Because of the concentration gradient, acrylamide monomers from the masked region diffuse into the UV exposed region and subsequently become cross-linked near the illumination interface, leading to a smaller than desired pore-size near the edge of the exposed region. Illumination power affects the rate monomers are consumed in the illuminated region as well as the rate monomers diffusing from the masked region are incorporated into the growing polymer chain. Therefore, reducing the illumination power should mitigate nonideal pore-size variation at the interface by (1) reducing the amount of monomers diffusing into the exposed region and (2) allowing incoming monomers to

(44) Fuxman, A. M.; McAuley, K. B.; Schreiner, L. J. *Chem. Eng. Sci.* **2005**, *60*, 1277–1293.

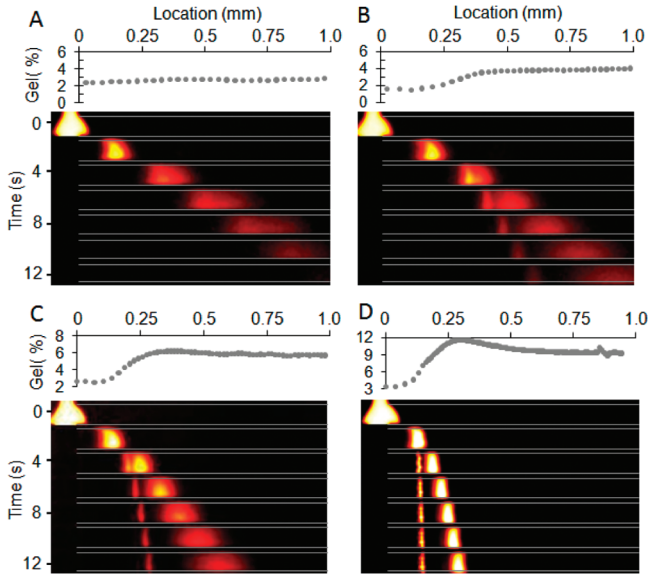

Figure 3. Discontinuous gel optimization yields decrease in separation length required for the CRP immunoassay: CRP assay on (A) 2.5/2.5%T, (B) 2.5/3.5%T, (C) 2.5/5%T, (D) 2.5/8%T discontinuous gel. E = 102 V/cm, [anti-CRP Ab*] = 66 nM, [CRP] = 16 nM.

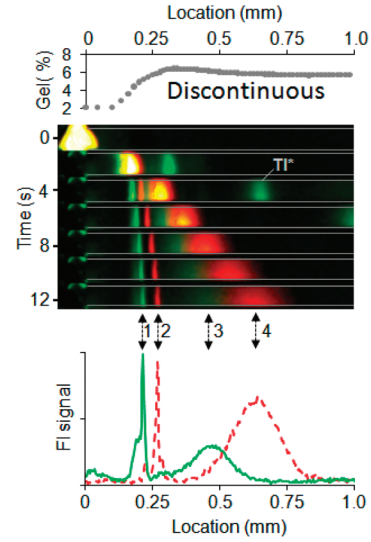

Figure 4. Two-color detection enables concurrent immunoassays for TNF-α and CRP in a discontinuous 2.5/5%T PA gel. Effective gel pore-size along the separation axis (top panel). Fluorescence images from the concurrent assays are shown for the first 12 s of the separation (false color, middle panel). Fluorescence intensity profiles are shown at 12 s for both immunoassays (bottom panel). E = 102 V/cm. Labels indicate (1) TNF-α complex; (2) CRP complex; (3) anti-TNF-α Ab*; (4) anti-CRP Ab*. [TI*] = 50 nM, [anti-CRP Ab*] = 66 nM, [CRP] = 16 nM, [anti-TNF-α Ab*] = 68 nM, [TNF-α] = 22 nM.

diffuse for longer distance before being cross-linked into the growing polymer chain.

To reduce the illumination power, various combinations of metallic-coated neutral density filters (1%, 10%, 25% 30%, or 50% from Omega Optical) were used. Filters were inserted in the IX-50 light path between the mercury arc lamp and the 4× UV objective. Further empirical optimization of the discontinuous gel fabrication protocol described in the Materials and Methods section identified an attenuated power of 1.25% total transmission using the 10%, 25%, and 50% filters and an adjusted exposure time of 3.3 min as optimal. In this case, power exiting the UV objective was approximately 7.5 mW/cm^2. Figure 2B presents the spatial pore-size variation along the separation axis for discontinuous gels fabricated using the modified partial illumination approach. The modified partial illumination approach yielded an interface with an effective 6%T pore-size, much larger pores than resulted from the initial partial illumination fabrication protocol; no exclusion of immune complex was observed for the selected precursor concentration. As can be observed aft of the interface, the modified partial illumination approach also yielded a more uniform pore-size separation gel, yielding significantly less "destacking" behavior for analyte bands migrating along the separation axis. Thus, all discontinuous gels described here utilized the attenuated partial illumination instrument.

Electrophoretic Immunoassay Optimization on the Discontinuous PA Gels. To minimize the separation length and time required to achieve baseline resolution between the antibody and immune complex, a series of discontinuous separation gels having progressively more pronounced pore-size transitions were analyzed (Figure 3). Table 1 summarizes the separation performance for the series of discontinuous gels studied, all with a pore-size discontinuity located ~200 μm downstream of the injection junction in the separation channel. Small pore-size gels in the separation channel enhanced $\Delta\mu/\mu_{Ab}$ and, in turn, reduced the separation length needed to achieve SR ≥ 1. For example, comparison of a 2.5/3.5%T discontinuous gel and a 2.5%/6%T gel show a 3× reduction in the separation length, resulting in a total separation length of 335 μm for the discontinuous 6%T separation gel. A commensurate reduction in the elapsed separation time needed was also observed. Building on the optimization study, a two-color homogeneous immunoassay was subsequently developed to complete on a 2.5/5%T discontinuous gel (Figure 4). An SR ≥ 1 was achieved for CRP in a separation length of 330 μm and an elapsed separation time of 3.6 s; while for TNF-α the separation was completed in 310 μm and 4 s. With the use of the discontinuous gel format, both immune complexes were resolved from their respective free antibodies by 150 μm aft of the 2.5/5%T gel interface. A 2.5/5%T discontinuous gel yields immunoassays that complete with a nearly 3× reduction in separation length and assay duration compared to a 2.5%T-to-8%T gradient gel (Figure 5). Spectral multiplexing is also key to achieving a short separation length for multianalyte assays by resolving spatially overlapped analyte peaks in a single channel (Figure 5B).

Adapting Discontinuous Gels for Single-Point Detection. To develop the discontinuous gels for homogeneous electrophoretic immunoassays compatible with PMT based single-point detection, the detector location for simultaneous two-color immunoassays was optimized through consideration of SR and assay duration. Importantly, slowly migrating species increase assay duration for single-point detection. In contrast, full field detection reduces the importance of slowly migrating species in determining total assay time, as all species within the field of view are imaged at every time point. If using full field detection, separation gel pore-size can be further decreased to reduce the separation length required to achieve SR > 1. Figure 3D illustrates a CRP immunoassay performed on a 2.5/8%T discontinuous gel where SR > 1 was achieved in just 3 s in a separation length of 188 μm. SR > 1.5 is achieved within 4 s and a separation length of 200 μm. CRP

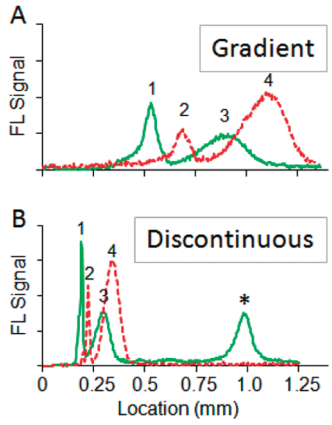

Figure 5. Discontinuous gel significantly decreases separation length required to achieve similar SR for two-color assays: (A) gradient gel axial fluorescence intensity profile taken 12.5 s after injection: SR for TNF assay, 1.24; SR for CRP assay, 1.39. (B) Discontinuous gel axial fluorescence intensity profile taken at 5.3 s after injection: SR for TNF assay, 1.27; SR for CRP assay, 1.43. E = 102 V/cm (first 5.5 s of separation) and E = 200 V/cm. Fluorescence intensity normalized by loading channel intensity. Labels indicate (1) TNF complex; (2) CRP complex; (3) anti-TNF Ab*; (4) anti-CRP Ab*. The * symbol indicates TI*, an internal standard.

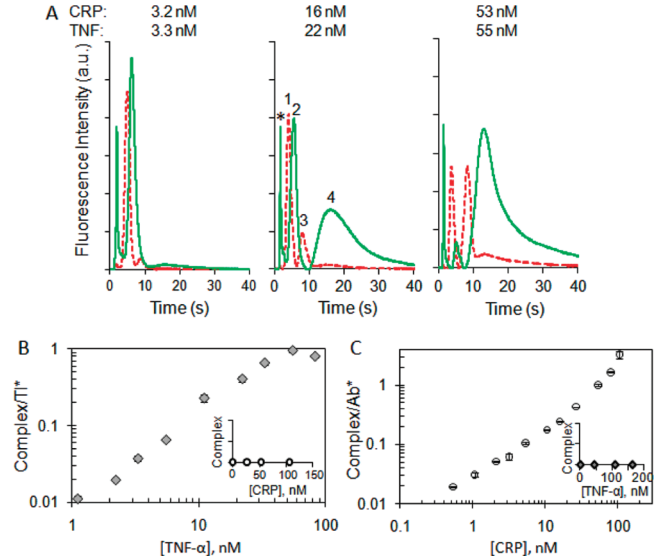

Figure 7. Two-color immunoassay is quantitative. (A) Electropherogram generated on a discontinuous gel with incubates containing CRP = 3.2 nM/TNF = 3.3nM, CRP = 16 nM/TNF = 22 nM, CRP = 53 nM/TNF = 55 nM. Labels indicate (1) anti-CRP Ab*; (2) anti-TNF Ab*; (3) CRP complex; (4) TNF complex. The * symbol indicates TI*, an internal standard. (B) TNF-α assay dose response curve with lower limit of detection (LLOD) of 2.2 nM (40 ng/mL), (C) CRP assay dose response curve with LLOD of 500 pM (11.5 ng/mL). Error bars denote standard deviation based on 3−5 runs; detection at 270 μm; E = 102 V/cm (first 5.5 s) and E = 200 V/cm.

immune complex was excluded at gel discontinuities with T > 8%. For these small pore-size gels, antibody migrated through the discontinuity thus maximizing the mobility difference ($\Delta\mu/\mu$). Exclusion of immune complex has previously aided homogeneous immunoassay completion, most often in conjunction with full-field scientific-grade CCD imaging.[24,45] Because of the expense and size of CCD cameras, single-point detection is preferred for point-of-care instruments.

As both TNF-α and CRP immune complexes could enter the separation gel, 2.5/5%T discontinuous gels were chosen for simultaneous single-point detection studies. Additionally, as species were not immobilized in the separation gel, the 5%T pore-size allowed sequential injections and separations, making the separation format compatible with both continuous monitoring assays and chip reuse in clinical settings. The required separation length for single-point detection is defined as the detector location resulting in well-resolved species peaks (SR > 1). With the use of CCD separation images, peak center and peak width (4σ spread indicated by error bars) were tracked as a function of time for both the CRP free antibody and immune complex peaks (Figure 6). As described, at the 5.5 s elapsed separation time point a two-step pull back voltage program was implemented to increase the separation electric field from 102 to 200 V/cm. The change in electric field can be observed as a shift in the slope of migration distance vs time for the discontinuous gel (middle panel, Figure 6). SR ~ 1.5 was achieved at an elapsed separation time of 5.6 s for discontinuous gels and at 13.2 s for gradient gels (right panel, Figure 6). At an SR ~ 1.5, the minimum between the two peaks informs selection of the optimal detector location which yields well-resolved electropherograms. With the use of this approach, the single-point detector was placed at ~250 μm for the discontinuous gel (2.5/5%T) and ~800 μm for the decreasing pore-size gradient gel (2.5%T-to-8%T). As compared to the gradient gel architecture, the discontinuous gel format achieved a 3× reduction in separation distance when using single-point detection.

Simultaneous Quantitation of CRP and TNF-α in a Single Channel. Simultaneous detection of TNF-α and CRP was implemented on the 2.5/5%T discontinuous gel using two-color single-point PMT detection (Figure 7A). A injector-to-detector length of 270 μm was estimated by first extracting the times required for antibody and complex migration to the detector (from electropherograms) and then obtaining analyte migration distance from

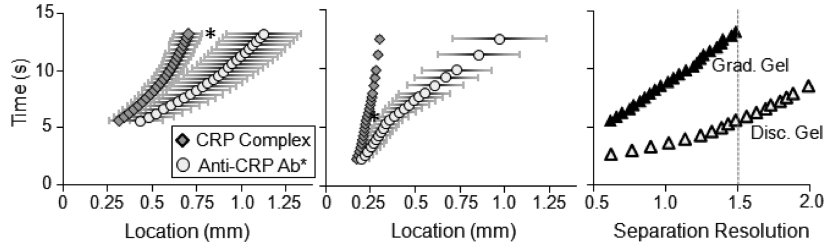

Figure 6. Single-point detector location optimization through determination of baseline separation conditions. Analysis of anti-CRP Ab* and CRP complex peak migration and peak widths for gradient gel (left panel) and 2.5/5% discontinuous gel (middle panel). Right panel: separation resolution for gradient and discontinuous gel formats vs time. Optimal single point detector location is indicated as *. E = 102 V/cm (first 5.5 s) and E = 200 V/cm.

CCD image sequences at the same migration times (Figure 6, middle panel for CRP assay). Dose response curves for CRP and TNF-α (Figure 7B,C) showed a quantitative capability with a lower limit of detection for the CRP assay of 11.5 ng/mL and a lower limit of detection for TNF-α assay of 40 ng/mL. No notable cross-reactivity between the TNF-α protein and the CRP antibody or for the CRP protein and TNF-α antibody was observed in the concurrent assay (insets of Figure 7B,C). Assay reproducibility was evaluated by conducting 10 sequential CRP immunoassays over a 20 min period. As shown in Figure S-1 in the Supporting Information, antibody peak migration exhibited a % RSD of 2.5% and the complex peak migration % RSD was 2.2%. The % RSD for the SR was 1.0%, and the antibody-to-complex peak height ratio exhibited a 2.7% RSD. The reproducibility performance is expected, as polyacrylamide gels exhibit low nonspecific adsorption and separation gel pore-size was properly selected to allow unrestricted migration of analyte species.

CONCLUSIONS

A systematic approach to assay development allows us to optimize the homogeneous electrophoretic immunoassay performance. In particular, on-chip discontinuous gels were introduced to enhance antibody and complex mobility differences, hence, achieving assay completion in an ultrashort separation distance. Further, spectral multiplexing and concurrent two-color detection is key to maintain short separation length for quantifying multiple biomarkers. Using CRP and TNF-α as model biomarkers, we demonstrate assay completion within 350 μm. Importantly, short separation lengths enable sufficient applied electric field strengths for rapid electrophoresis, with low applied electrical potential requirements; for the discontinuous gels demonstrated here, an applied electric field strength of 100 V/cm would require 3.5 V across the required separation length. In optimizing discontinuous pore-size gels for both full field imaging and single-point detection, we introduce an improved partial illumination approach that results in well-controlled gel pore-size fabrication via mask-based in situ photopolymerization. While developed for the discontinuous separation gels, the approach is widely applicable to fabrication of various functional polymer units (e.g., membranes, filters) in microfluidic channels. Using spectral multiplexing, we demonstrate simultaneous immunoassays for CRP and TNF-α as quantitative with no appreciable cross-reactivity for the targets considered.

With the use of the design approach described, homogeneous electrophoretic immunoassays for other protein biomarkers can be optimized through tuning the sieving matrix pore-size to generate sufficient mobility differences between the antibody and immune complex. Further separation length reductions (<200 μm) can be achieved by excluding the immune complex from the separation gel, which is applicable for implementation with full-field imaging. However, single-point detection is often desired for low-cost point-of-care diagnostic instruments, thus separation gels allowing entry of immune complexes were the focus of this study. Revisions to chip designs to realize portable diagnostic instruments using high electric field strength electrophoresis, yet operated under low applied voltages (<9 V), are underway by our group. While further system-level integration is also underway, the discontinuous gel sieving matrix architecture introduced here forms a key step toward realizing battery-operated electrophoresis systems for quantitation of protein biomarkers in near-patient environments.

(45) Reichmuth, D. S.; Wang, S. K.; Barrett, L. M.; Throckmorton, D. J.; Einfeld, W.; Singh, A. K. *Lab Chip* **2008**, *8*, 1319–1324.

ACKNOWLEDGMENT

The authors thank the Hellman Family Faculty Award at UC Berkeley for generous financial support, as well as Caliper Life Sciences for glass chip and equipment support. The authors thank Ms. Kelly Karns and Dr. Mei He for assistance. C.H. is a National Science Foundation Graduate Research Fellow. A.E.H. is a DARPA Young Faculty Awardee and Alfred P. Sloan Research Fellow in chemistry.

SUPPORTING INFORMATION AVAILABLE

Additional information as noted in text. This material is available free of charge via the Internet at http://pubs.acs.org.

Received for review January 21, 2010. Accepted March 8, 2010.

AC100182J